International Journal of Innovative
Computing, Information and Control
Volume 8, Number 7(B), July 2012

 ISSN 1349-4198
pp. 5149–5164

SURFACE REFLECTANCE COMPONENTS SEPARATION FROM SINGLE COLOR IMAGES USING THE MEAN-SHIFT DECOMPOSITION TECHNIQUE

Mouncef Lahlou and Malek Adjouadi

Department of Electrical and Computer Engineering
College of Engineering and Computing
Florida International University
10555 West Flagler Street, Miami, FL 33174, USA
{mouncef.lahlou1; adjouadi}@fiu.edu

Received March 2011; revised October 2011

Abstract. *This study provides a resolution to the separation of specular and diffuse reflectance components in images of textured scenes. The proposed method can be used to solve several challenging tasks associated with computer vision applications ranging from specularity removal, image filtering, and surface reconstruction. We present a unified framework to achieve object surface reflectance separation by studying the dissimilarities between the reflectance components distribution in scene images delineated on a normalized color space. A simple but robust reflectance decomposition technique is introduced based on the Eigen-decomposition transform we named the Mean-Shift Decomposition (MSD) method. This technique provides a direct access to surface shape information through diffuse shading pixels isolation. In addition, the proposed method does not require any local color segmentation process as it differentiates between both reflectance components efficiently. This is viewed as a significant contribution to the prevailing approach of several proposed methods in the literature that operate on images by aggregating color information along each image plane. To recover objects surface geometry information, we formulate a specularity removal process by shifting the specular reflectance components toward the decomposed diffuse reflectance distribution. An empirical evaluation of the proposed reflectance separation technique is performed on several images comprising uniform color surfaces, multicolor surfaces, and highly textured surfaces.*
Keywords: Reflection separation, Shape invariants, Specular reflection removal, Surface reconstruction, Image restoration, Dichromatic reflection model

1. **Introduction.** In computer vision, the modeling of surface reflectance is a topic of vital importance for purposes involving surface analysis and image understanding. By separating objects surface reflectance properties, powerful Lambertian-based methods can be applied for tracking, classification, reconstruction and recognition accurately to real-world scenarios [1]. Scenarios are assumed by many algorithms to consist only of diffuse reflections while specular ones are considered in many occasions to be negligible. Specular reflections confuse many vision problems since they produce image attributes that do not bind directly with intrinsic surface properties such as shape and spectral reflectance. Thus, methods that successfully separate both reflectance components in images are desired to advance current and future methods that do or will suffer from this complex reflectance occurrence.

This paper addresses the separation of reflection components in scene images as means to improve the effectiveness of the aforementioned applications. Unlike many of the existing methods, which limit their application to the reflectance component [2,3], our approach considers analyzing the image intrinsic properties relating to both diffuse and

specular reflectance components. We restrict our consideration to surfaces that are well represented by the dichromatic reflectance model introduced by Shafer [4]. This model suggests the possibility of decomposing surfaces into two-distinct reflectance constituents solely based on color image information. Our approach studies the dissimilarities between the diffuse and specular reflectance distributions projected in a normalized color space in order to isolate information about the material properties in an image scene while preserving the surface geometry information.

We introduce a simple but efficient reflectance decomposition technique based on the Eigen-decomposition transform that we refer to as the Mean-Shift Decomposition (MSD) method. This technique provides a direct access to surface shape information through diffuse shading pixels seclusion. In addition, the proposed method does not require any local color segmentation process as it differentiates between both reflectance components through the proposed MSD method which differs from several proposed methods in the literature that operate by aggregating color information along each image plane.

The contributions involved in the proposed reflectance separation method reside in:

- Analyzing and separating the image reflectance component using the Mean-shift decomposition technique derived based on the Eigen-decomposition transform.
- Recovering the surface geometry information by isolating the image diffuse reflectance distribution.
- Formulating a specular reflectance removal process by shifting the specular reflectance components toward the decomposed diffuse reflectance distribution.
- Evaluating the proposed algorithm on several images comprising uniform color surfaces, multicolor surfaces, and highly textured surfaces.

The rest of the paper is organized as follows. We begin by introducing a literature review on different related methods used for accomplishing the diffuse/specular separation task as summarized in Section 2. In Section 3, a review is given on several types of reflectance models used for reflection measurements. This same section also describes the model as employed in the reflectance separation approach considered in this study. Section 4 presents the chromaticity-color space used as a basis to the MSD technique. Sections 5 and 6 describe the classification of the image reflectance components using the MSD method and the specular removal process, respectively. An outline of the proposed algorithm implementation is presented in Section 7. Finally, we evaluate and summarize our proposed method in Sections 8 and 9.

2. **Related Work.**

Many methods have been proposed for separating reflection components using single or multiple input images of non-Lambertian objects (these are objects that deviate from the Lambert Law which assumes that luminance of a diffuse surface is the same in all directions; as formulated in 1760 by J. Lambert).

Based on color and image intensities, Sato and Ikeuchi [5] introduced a four-dimensional temporal-color space to analyze the diffuse and specular reflections. Their method has the ability to separate the reflection components using local interactions; however, it requires numerous input images with variation of illuminant directions. The benefit of using local analysis is that it admits highly textured scenes that do not contain piecewise constant diffuse colors. Lin et al. [6] used color histogram differencing to identify specular reflectance with multi-baseline stereo-vision. Their method makes use of the image pixel color stability to the field of view changes, since colors of specular pixels are dependent on the scene viewing positions while the diffuse pixel colors are not. Lin and Shum [7] introduced a method that uses several sparse images registered under different illumination positions. Their method uses the neutral interface reflection model that combines finite

dimensional basis functions [8] and the dichromatic reflectance model [4] to form a closed form linear surface reflectance.

Other methods based on multiple input images make use of extrinsic cues such as polarizing filters to enable the recovery of a spatially-varying source colors [9,10]. Wolff and Boult [11] used a polarizing filter to separate both specular and diffuse reflection components from grey images. They noticed that diffuse reflections tend to be less polarized than the specular reflections along most incident reflection angles. On the other hand, reflectance separation methods that use a single input image have also attracted several considerations from the research community. Shafer [4] introduced the dichromatic reflectance model suggesting the ability of decomposing an image into its specular and diffuse components based on the parallelogram distribution of colors in RGB space. Klinker et al. [12] showed that the color histogram of the image diffuse reflection color forms a T-shaped distribution when the diffuse colors are the same along each point on an objects surface. The color distribution they proposed forms linear clusters representing the diffuse and specular pixels. By separating these clusters, the image becomes segmented into several regions of homogeneous reflectance color. Later, Tan et al. [13] iteratively compared the intensity logarithmic differentiation of an input image and its specular-free image. Their method reduced the specular component value of each pixel iteratively by considering one of its neighbor pixels as having a similar diffuse component characteristic. Mallick et al. [14] applied a family of partial differential equations (PDE) that iteratively erodes the specular reflectance component at each pixel. Similarly, Khosrayy et al. [15] presented a method based on PDF-matched measure of short-term linear image signal prediction. The image source signals (i.e., image reflectance) are recovered by finding an un-mixing matrix that maximizes the predictability of each extracted surface reflectance.

3. **Reflection Model and Image Formation.** The use of physical reflectance measurements has shown to benefit the rendering of surface reflectance effectively. Such measurements can provide an ideal choice of parameters for existing reflectance models and can be used also to provide the basis for entirely other new reflectance models. For instance, the bidirectional reflectance distribution function (BRDF) measurement describes the reflection of an opaque surface by measuring the ratio of the radiance L reflected from the surface in a certain direction to the incident irradiance I at a particular wavelength λ. We consider the BRDF to be a five-dimensional function of wavelength and imaging geometry, whose measurement function f can be described as:

$$f(\Theta, \lambda) = \frac{dL(\theta_r, \phi_r)}{dI(\theta_i, \phi_i)} \tag{1}$$

where $\Theta = (\theta_i, \phi_i, \theta_r, \phi_r)$ defines the directions of the incident and reflected radiance in the local spherical coordinate system. A simple model that can be generated from the BRDF measurement is the Lambertian reflectance model where the BRDF is a constant function of the imaging geometry so that $f(\Theta, \lambda) = f(\lambda)$. Another common BRDF model is the dichromatic model of reflectance derived by Shafer [4] to represent dielectric materials. According to this model, the BRDF of the surface can be decomposed into two additive components: (1) the specular reflectance representing the surface interface, and (2) the diffuse reflectance representing the surface body. This model assumes that each reflectance component can be expressed as being a function of wavelength and imaging geometry, which leads to the following expression of the dichromatic BRDF model observed from a surface point n:

$$f(n, \lambda) = m_d(n) S_d(n, \lambda) E(n, \lambda) + m_s(n) S_s(n, \lambda) E(n, \lambda) \tag{2}$$

where m_d and m_s are the geometrical scale factors for the diffuse and specular reflectance, respectively, which depend on the surface properties and illumination geometry Θ. The S_d and S_s components are the diffuse spectral reflectance function and the specular spectral reflectance function, respectively, while E is the spectral distribution function of the illuminant, and n is the position of the surface point in a three-dimensional coordinate system.

Most methods that operate on dielectric inhomogeneous objects use the neutral interface reflection assumption (NIR) introduced by Lee et al. [16]. This assumption suggests that the spectral reflectance distribution of the specular reflection component S_s is similar to the spectral energy distribution of the incident light E, [17-19]. As a result of this assumption Equation (2) can now be expressed as follows:

$$f(n,\lambda) = m_d(n)S_d(n,\lambda)E(n,\lambda) + m_s(n)E(n,\lambda) \tag{3}$$

By combining the dichromatic reflectance model represented by Equation (3) with the camera intrinsic properties, the image formation equation for a surface element illuminated by a light source is described as follows:

$$\rho_k(n) = m_d(n)D_k(n) + m_s(n)S_k(n) \tag{4}$$

where $D_k(n) = \int_\Omega S_d(n,\lambda)E(n,\lambda)C_k(\lambda)d\lambda$ and $S_k(n) = \int_\Omega E(n,\lambda)C_k(\lambda)d\lambda$. Here $\rho_k = \{\rho_r, \rho_g, \rho_b\}$ is the RGB color vector response from a typical camera consisting of $k = \{r, g, b\}$ measurements, and $C_k = \{C_r, C_g, C_b\}$ is the sensor sensitivity of the three color channels over the range of the visible spectrum Ω. D_k and S_k are the diffuse and specular image components and are assumed to be unit length vectors $||D_k|| = ||S_k|| = 1$.

Even though the dichromatic model was originally established to process materials such as glass, plastics, cloths, or even plant leaves, the model has also shown to be useful for applications involving human skin [20-22].

Throughout this paper, we use the BRDF dichromatic model described in Equation (4), and we assume that the illumination spectral power distribution is formed using a single and uniform illumination color $E(\lambda)$ independent from the image coordinates n. We note that the camera properties employed for image formation ignores the read noise and gain factor.

4. **Image-Chromaticity Color Space.**

Color space transformations have shown to help exploring the knowledge of the illuminant attributes in color images which results in describing the image diffuse information independently [23-25]. By shifting or projecting image intensities into a specified color space, depending on the motivated application, one can linearly combine the three image color channels to obtain either one or two distinct diffuse channels. Zickler et al. [24] proposed a color space referred to as *SUV color space* that isolates two-predominantly diffuse channels while retaining the entire specular components information apart. Similarly, Park [23] isolated the diffuse reflectance channels while maintaining a similarity to the *HSI color space* using a linear transformation described by a matrix L and a rotational transformation represented by a matrix R. The two matrices, L and R, are chosen in a way that the third axis of the image color is aligned with the illumination color vector; this reveals an image channel highly insensitive to specular reflections and other two channels consisting mainly of diffuse components. On the other hand, Tan et al. [13] obtained a specular free image channel using a source dependent non-linear transformation of the RGB space. This transformation yields a positive monochromatic image that depends directly on diffuse shading information. Similar to

Tan and colleagues method, Yoon and Kweon [26] proposed another non-linear transformation strictly relied on white illumination that produces also a positive grayscale image dominated by diffuse reflectance components and independent from specular effects.

In this study, we consider a different approach from the color transformation methods discussed. It is important to analyze the reflectance components distribution in the RGB color space to efficiently describe the correlation between those two reflection constituents. As mentioned in the previous section, assuming a dichromatic model object, the spectral reflectance distribution of the specular reflection component is similar to the spectral energy distribution of the incident light. Tan et al. [27] introduced a new space transformation to analyze the relationship between illumination color and image intensity identified as *inverse-intensity chromaticity space (IIC)*. Initiated mainly for illumination color estimation, we base our method on the *IIC*-space to identify the image pixels representing the diffuse and specular reflections. By projecting an RGB image into the *IIC*-space, the distribution of the image reflectance forms a set of straight lines expressed by the following equation:

$$\sigma_k = r\frac{1}{\sum_{j\in k}\rho_j(n)} + \omega_{s,k}(n) \tag{5}$$

where $r = m_d(n)(\omega_{d,k}(n) - \omega_{s,k}(n))$. Here, σ_k is the image intensity chromaticity of ρ_k, $\omega_{d,k}$ and $\omega_{s,k}$ are the diffuse and specular reflectance chromaticities of D_k and S_k respectively. Figures 1(b) and 1(c) show the distribution of the image green-channel projected on the *IIC*-space. These straight lines portraying both reflection components consist of several sets of different m_d values representing the geometrical surface properties of the diffuse reflectance. These values depict the orientation of the reflection lines since they are associated with the gradient r in Equation (5). It can be observed empirically that as the object surface texture measurement is small (i.e., smooth surface), the diffuse reflectance distribution characterized in the *IIC*-space is relatively dense and is prone to merge with the specular reflectance components. However, if the object surface texture measurement is large (i.e., rough surface), the diffuse reflectance distribution becomes instead relatively sparse. Therefore, by understanding the distribution of the image reflectance properties in the *IIC*-space, the specular/diffuse separation process can be accomplished by finding the maximum reflectance disparities between the image pixels representing the specular and diffuse reflections.

In the next section, we describe how these reflection lines differences can be categorized to separate the image diffuse and specular components using a simple method based on the Eigen-decomposition transformation, we call *Mean-Shift Decomposition (MSD)*.

5. **Image Reflectance Components Classification.** The ability to determine the specular highlight regions has always been an ill-posed problem for several specular/diffuse separation methods. Previously, some methods require explicit color segmentation techniques to handle specular regions in multicolored surfaces especially when dealing with objects having highly textured surfaces and when processing single input images. In comparison with those methods, our proposed technique finds the maximum variance of image reflectance pixels to isolate both reflectance component distributions distinctly. This section introduces the *Mean-shift decomposition method*, a simple technique for specular and diffuse reflectance distribution classification over the *IIC*-space based on the Eigen-decomposition transform. Here we consider a two-class problem where the classes are labeled to describe a diffuse reflectance class or a specular reflectance class.

Consider a vector $x_i : R^2 \to [0, 1]$ where $i = 1, 2, \ldots, N$, representing a sample point of the image reflectance components projected on the *IIC*-space and a matrix X denoting

a set of all N points $X = [x_1, x_2, \ldots, x_N]$. Our objective is to find a separation line that maximizes the variance of the projected reflectance data. Let U denote the direction of this line defining a new orthonormal basis of the projected reflectance values. These points can be expressed such that:

$$Y = U^T X \tag{6}$$

where $Y = [y_1, y_2, \ldots, y_N]$ denotes the coordinates of the reflection points in the new basis, here we choose $U^T U = 1$ as a constrain to maximize the reflectance variance. The mean of the projected reflectance components into the new basis line is $U^T \bar{X}$ where $\bar{X}$ is the sample set mean given by:

$$\bar{X} = \frac{1}{N} \sum_{i=1}^{N} X_i \tag{7}$$

and the variance of the image reflectance components is given by:

$$var(X) = \frac{1}{N} \sum_{i=1}^{N} \left\{ U^T X_i - U^T \bar{X}_i \right\}^2 = U^T C U \tag{8}$$

where C is the image reflection components covariance matrix defined as:

$$C = \frac{1}{N} \sum_{i=1}^{N} (X_i - \bar{X})(X_i - \bar{X})^T \tag{9}$$

By maximizing the projected variance in Equation (8) with respect to U, the new orthogonal basis is represented by the eigenvectors of the covariance matrix C such that:

$$CU = \Lambda U \tag{10}$$

where Λ is a diagonal matrix of decreasing eigenvalues and U is an orthonormal matrix of corresponding eigenvectors. The maximum variance separating the image diffuse and specular reflectance is obtained when the vector U corresponds to the highest eigenvalue. It is clear that the line separating the reflectance components into diffuse and specular reflections intersects both reflection distributions and is oriented according to the direction variations of the straight lines obtained by projecting the image into the *IIC*-space.

The *MSD* method finds the correlated features associated with each reflectance components mainly promoted in the center of the projected image cluster. This correlation occurring between both reflectance distributions rises for the fact that the image reflectance components projected on the *IIC*-space are characterized according to the image intensities distribution. Therefore, shifting the separation line represented by the direction of the new basis axis U to the center of the reflection distribution approximates the location that considerably relates both reflectance components in the *IIC*-space. The separation line is consequently shifted toward the center of the distance separating the diffuse and specular reflectance distributions means. We define the expression of the *MSD* separation line as:

$$f_k(n) = \tilde{u} \left(\frac{1}{\sum_{j \in k} \rho_j(n)} - \bar{x}_{1,k} \right) + \bar{x}_{2,k} \tag{11}$$

where the gradient $\tilde{u}$ denotes the direction derived from the eigenvector of the orthonormal basis U corresponding to the highest eigenvalue in Λ. $\bar{x}_{1,k}$ and $\bar{x}_{2,k}$ are the means of the projected image reflectance on the *IIC*-space corresponding to the matrix X. The proposed separation line in Equation (11) can efficiently partition the reflection distribution into two separate reflection classes as shown in Figure 1(d). Finally, the specular

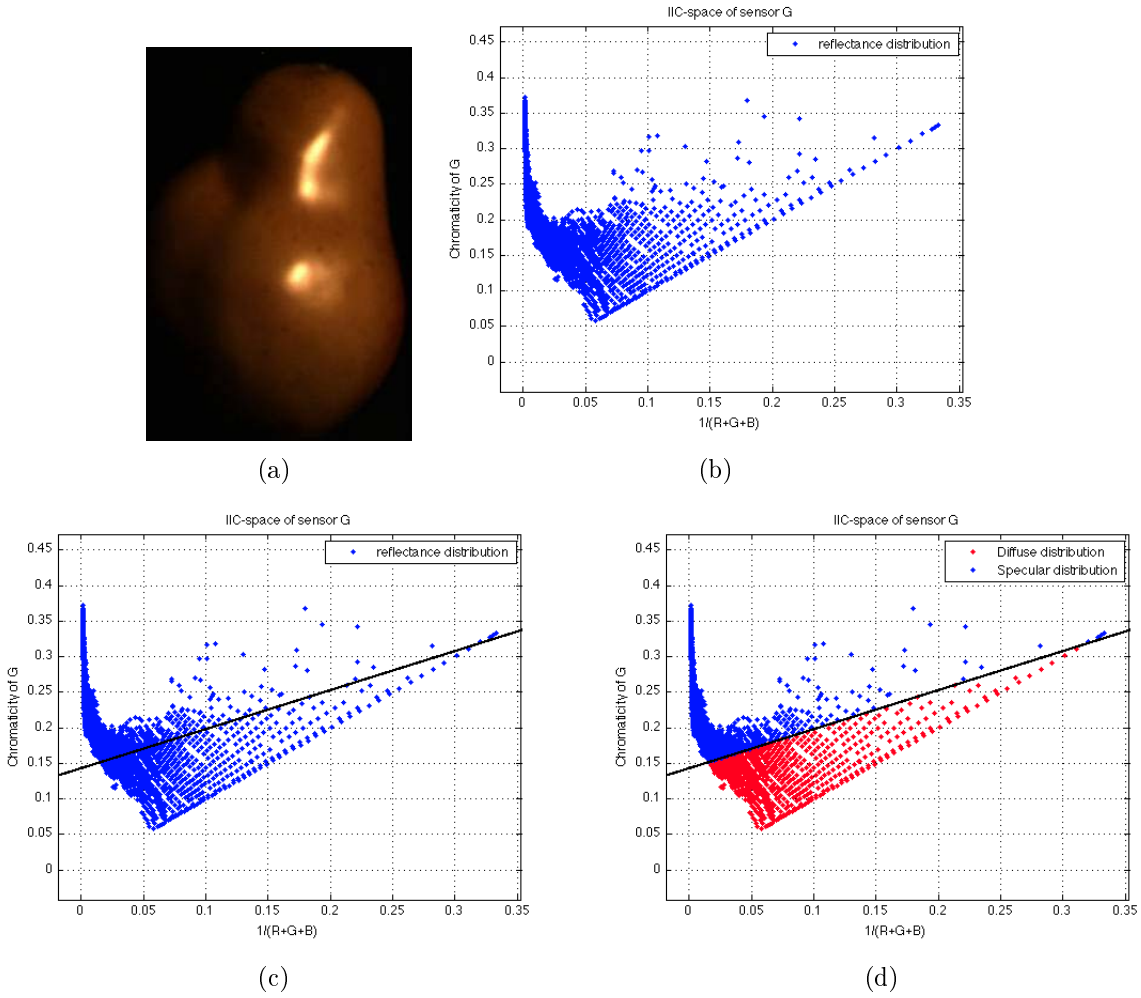

FIGURE 1. Reflectance distribution separation over the IIC-space. (a) Input image. (b) Mapping image intensities of (a) over the IIC-space. (c) Separating the reflectance distribution into two distinct classes using the separation line (black) obtained from the proposed MSD method. (d) Classification of the projected image reflectance into diffuse reflectance distribution (red) and specular reflectance distribution (blue).

reflection components represented in the image can now be easily located by mapping the mean value of the brightest specular blob into the IIC-space.

6. **Specular Reflection Removal.** The dichromatic reflectance model suggests the possibility of decomposing an image into its specular and diffuse components based on image color information. After locating the image pixels representing the image diffuse and specular reflectance using the approach proposed in the previous section, in this section, we recover the diffuse properties of the specular distribution components by shifting the specular reflectance distribution components within the diffuse reflectance distribution in the IIC-space. This process has the advantage of preserving the surface color information and the diffuse reflection properties encoded in the geometric scale factor m_d.

Finding the shifting distance between each specular element and its new diffuse value is an important process for robust diffuse reflectance estimation. Let $C_{i,k}$ where $i = 1, 2, \ldots, N$, denote the current specular reflection value projected on the IIC-space. And let $N_{i,k}$ denote the newly shifted $C_{i,k}$ into the diffuse reflectance distribution by a Euclidean

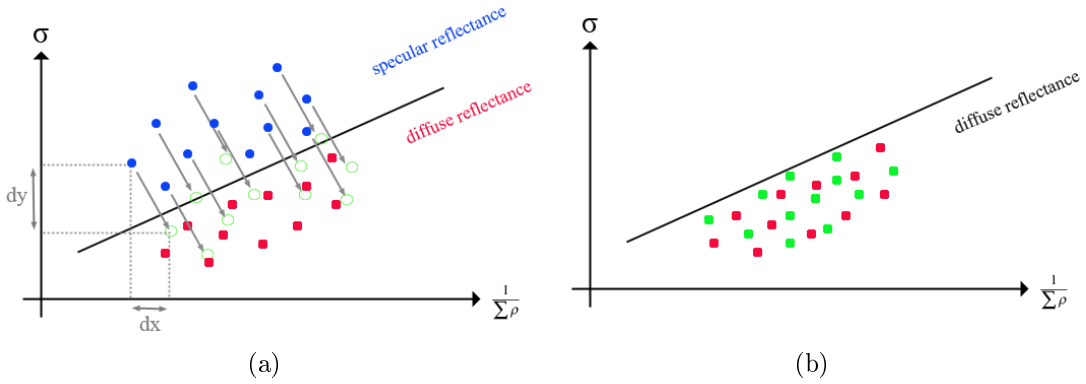

FIGURE 2. Specular reflectance shifting process: (a) specular reflectance components (blue-dotes) shifting toward the new projected value (green-circle) in the IIC-space, (b) specular reflectance new positioning (green-squares) within the diffuse reflection distribution

distance D_i expressed as:

$$D_i = (d_{i,x}^2 + d_{i,y}^2)^{1/2} \tag{12}$$

where $d_{i,x}$ and $d_{i,y}$ are the shifting distances over the inverse-intensity axis and image chromaticity respectively, Figure 2(a). We derive $d_{i,x}$ as follows:

$$d_{i,x} = \frac{1}{\sum_{j\in k} N_{i,j}} - \frac{1}{\sum_{j\in k} C_{i,j}} \tag{13}$$

$$d_{i,x} = \frac{1}{\sum_{j\in k} C_{i,j} - \varepsilon_k} - \frac{1}{\sum_{j\in k} C_{i,j}} \tag{14}$$

$$d_{i,x} = \frac{\varepsilon_k}{\sum_{j\in k} C_{i,j} \left(\sum_{j\in k} C_{i,j} - \varepsilon_k\right)} \tag{15}$$

and $d_{i,y}$ as follows:

$$d_{i,y} = \frac{C_{i,k}}{\sum_{j\in k} C_{i,j}} - \frac{N_{i,k}}{\sum_{j\in k} N_{i,j}} \tag{16}$$

$$d_{i,y} = \frac{C_{i,k}}{\sum_{j\in k} C_{i,j}} - \frac{C_{i,k} - \varepsilon_k}{\sum_{j\in k} C_{i,j} - \varepsilon_k} \tag{17}$$

$$d_{i,y} = \frac{\varepsilon_k \left(\sum_{j\in k} C_{i,j} - C_{i,k}\right)}{\sum_{j\in k} C_{i,j} \left(\sum_{j\in k} C_{i,j} - \varepsilon_k\right)} \tag{18}$$

where the threshold ε defines the minimum value measured of $C_{i,k}$ and the difference of the maximum diffuse reflectance value of $D_{i,k}$ with respect to the minimum specular reflectance value of $S_{i,k}$, expressed as follows:

$$\varepsilon_k = (C_{i,k})_{\min} + (S_{i,k})_{\min} - (D_{i,k})_{\min} \tag{19}$$

The importance of Equation (12) is to shift the specular reflectance distribution towards the direction of the image elements representing the diffuse reflectance, the threshold specified in Equation (19) preserves the information of the surface geometry by adding the difference of both reflectance classes.

Algorithm 1 Specular reflection removal algorithm flow

Require: $I : \{I_R, I_G, I_B\}$ RGB image of N element
Ensure: I_{Spec} – Specular image components
Ensure: I_{Diff} – Diffuse image components
Ensure: $I_{SpecularFree}$ – Specular-free RGB image
1: $I_{InvSum} \leftarrow inverseSum(I_R, I_G, I_B)$
2: **for** $k \in R, G, B$ **do**
3: $\sigma_k \leftarrow imageChromaticity(I_k)$
4: $\bar{\mu}_{i,k} \leftarrow calculMean(\sigma_k, I_{InvSum})$ // Equation (7)
5: $C_k \leftarrow calculCovariance(\sigma_k, I_{InvSum})$ // Equation (9)
6: $\{\lambda_k, v_k\} \leftarrow eigenDecomposition(C_k)$// Equation (10)
7: $\{\tilde{\lambda}_k, \tilde{v}_k\} \leftarrow sortEigen(\lambda_k, v_k)$
8: $f_k \leftarrow lineSeparation(\tilde{v}_k, \bar{\mu}_{i,k})$
9: $I_{\max} \leftarrow maxBlob(I_k)$
10: $I_{Spec,k} \leftarrow \sigma_{\max} \in \sigma_k$
11: $I_{Diff,k} \leftarrow I_k \cap I_{Spec,k}$
12: **for** $n \in [1, N]$ **do**
13: $\varepsilon \leftarrow distanceThreshold(I_{Spec,k})$ // Equation (19)
14: $d_{n,x} \leftarrow shiftDx(\varepsilon)$ // Equation (15)
15: $d_{n,y} \leftarrow shiftDy(\varepsilon)$ // Equation (18)
16: $D_n \leftarrow shiftDist(d_{n,x}, d_{n,y})$ // Equation (12)
17: $\tilde{I}_{Spec,k} \leftarrow shiftSpec(I_{Spec,k}, D_n)$
18: **end for**
19: $I_k \leftarrow I_{Diff,k} \cup \tilde{I}_{Spec,k}$
20: **end for**
21: $I_{Diff} \leftarrow I_{Diff,R} \cup I_{Diff,G} \cup I_{Diff,B}$
22: $I_{Spec} \leftarrow I_{Spec,R} \cup I_{Spec,G} \cup I_{Spec,B}$
23: $I_{SpecularFree} \leftarrow I_R \cup I_G \cup I_B$

7. **Algorithm Implementation.** Algorithm 1 outlines the steps and general data flow (Figure 3) of the proposed specular reflectance decomposition algorithm described in this paper. The algorithm proceeds as follows. As a first stage, the input image intensities are mapped to the *IIC*-space by calculating the inverse-intensity sum and the image chromaticities for every channel k (line 1-3). The next step is to find a separation line that classifies each image intensity components into diffuse reflectance or specular reflectance. The means of the *IIC*-space coordinates representing the inverse image intensities and the image chromaticities are determined in order to find the image covariance matrix in Equation (9) (line 4-5) and to shift the separation line toward the center of the reflectance distribution (line 8).

A final step for obtaining the separation line is to calculate the gradient of line expression in Equation (11). After sorting the eigenvalues (line 7), the eigenvector direction of the highest eigenvalue is used as the gradient of the line separation equation. The next stage consists of finding the distance separating the targeted new location of the specular pixel in the diffuse reflectance distribution and its current location.

The distance along the inverse-intensity axis (line 14) and the image chromaticity (line 15) are calculated for every specular reflectance distribution constituent. The Euclidian distance in Equation (12) is then obtained before the specular value is shifted (line 16-17). Finally, the three processed RGB channels are combined to produce a specular-free image (line 23).

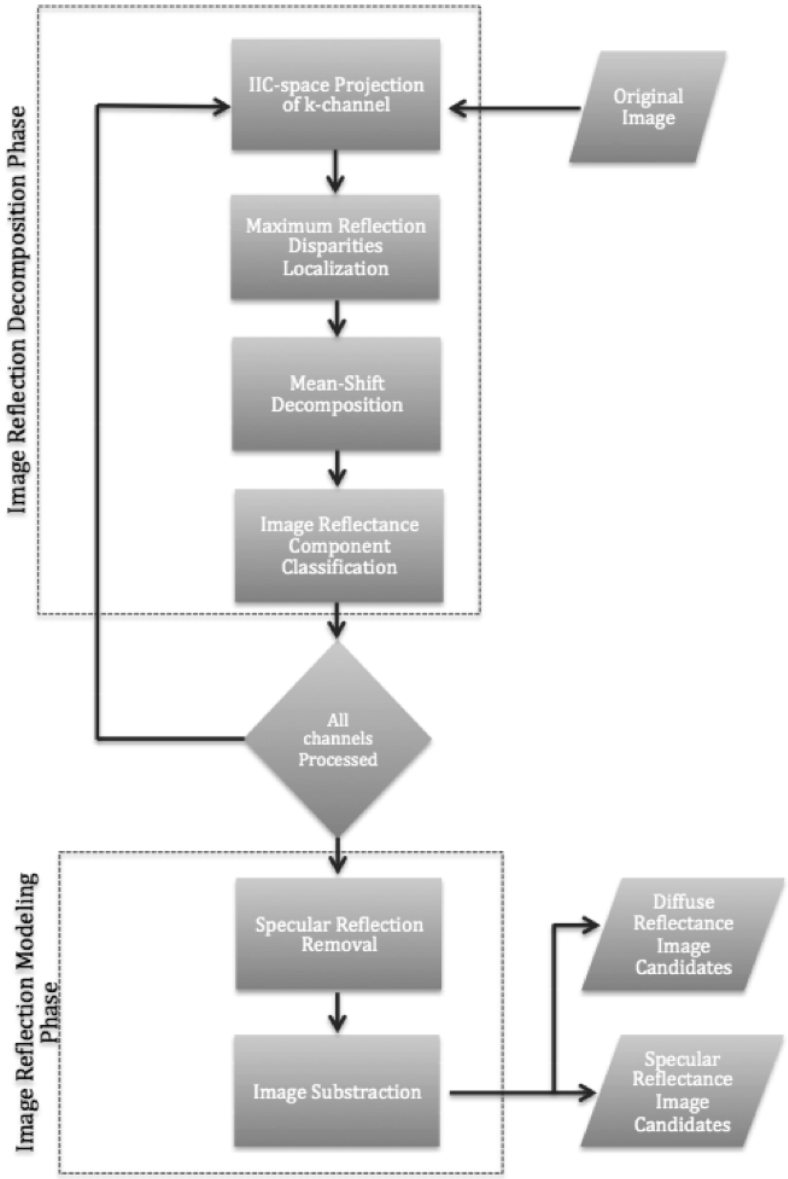

FIGURE 3. Flowchart of the proposed reflection decomposition method

8. **Experimental Results and Discussions.** The proposed method was evaluated using several real and synthetic images from the color image dataset used in [13]. Different image surfaces were targeted in our experiment especially images consisting of uniform colored surfaces, multicolored surfaces, and highly textured surfaces. The images were registered using a progressive 3-CCD digital camera SONY DXC-9000, by setting the camera correction option off. Also to ensure that the output of the camera is linear to the flux of incident light, a Photo Research PR-650 spectrometer was used for this task.

Figure 6 shows the results of recovering the diffuse image reflectance from a uniform surface color image. The obtained result is achieved using only two iterations and correctly handles all reflectance regions altered by the specular reflections. Also, since the proposed method processes each channel independently, all image color channels recovered the surface shape efficiently. The images in this case were processed without making use of

(a) (b) (c)

FIGURE 4. Reflection separation results: (a) input image, (b) separation result using our method, (c) separation result using Tan et al. method [13]

the illuminant color and by setting the calculated Euclidian distance D in Equation (12) to a constant value along all reflectance distribution components.

It is important to note that this practice of keeping D constant does well only on images with uniform color surfaces. However, for multicolored images, this distance has to be calculated independently for every specular reflectance component in order to achieve acceptable results. In Figure 7, cross-sections of all input image three-color channels are shown to describe the iteration process performance. The solid blue horizontal line in Figure 7(a) represents the cross-section area used to portray the iteration results in Figures 6(d)-6(f). In each iteration process, it is noticeable that the surface color tone is preserved and attempts to complete the signal shape of the diffuse reflectance components. On the third and fourth iteration, we notice the specular signal flattening on a nearly constant pixel value resulting in wrong reflectance component separation.

Another experiment performed on multicolored and significantly textured images is presented in Figure 5. Looking closely at the pear image in Figures 5(a)-5(c), we notice that the diffuse texture barely visible in the input image is exposed when the specular effects are removed. Similarly in Figures 5(d)-5(f), the fish texture is recovered while preserving the surface color of the object. Figures 5(g)-5(i) show the results of processing several object surfaces grouped in one single image. Some of the surfaces are effectively recovered such as the fish object and the dole with blue scarf; however, other objects such as the yellow ball and some of the monster figurine surface were still suffering from the specular reflection effects.

Finally, we compare our algorithm with one of the well-known specular/diffuse reflection separation methods in the literature proposed by Tan et al. [13] in Figure 4. The figure compares both methods' results applied to a 3D head object with a uniform surface color. Both the shape surface color and the surface shade properties were efficiently estimated using our proposed method, similarly to Tan's et al. method where the surface shape was effectively reconstructed and the specular reflections were well removed; however, the surface color was estimated inaccurately.

9. **Conclusions.** This paper presented a framework for specular and diffuse reflectance separation in color images based on a newly introduced Mean-shift decomposition technique. This approach relies mainly on image reflectance correlations in defining a suitable

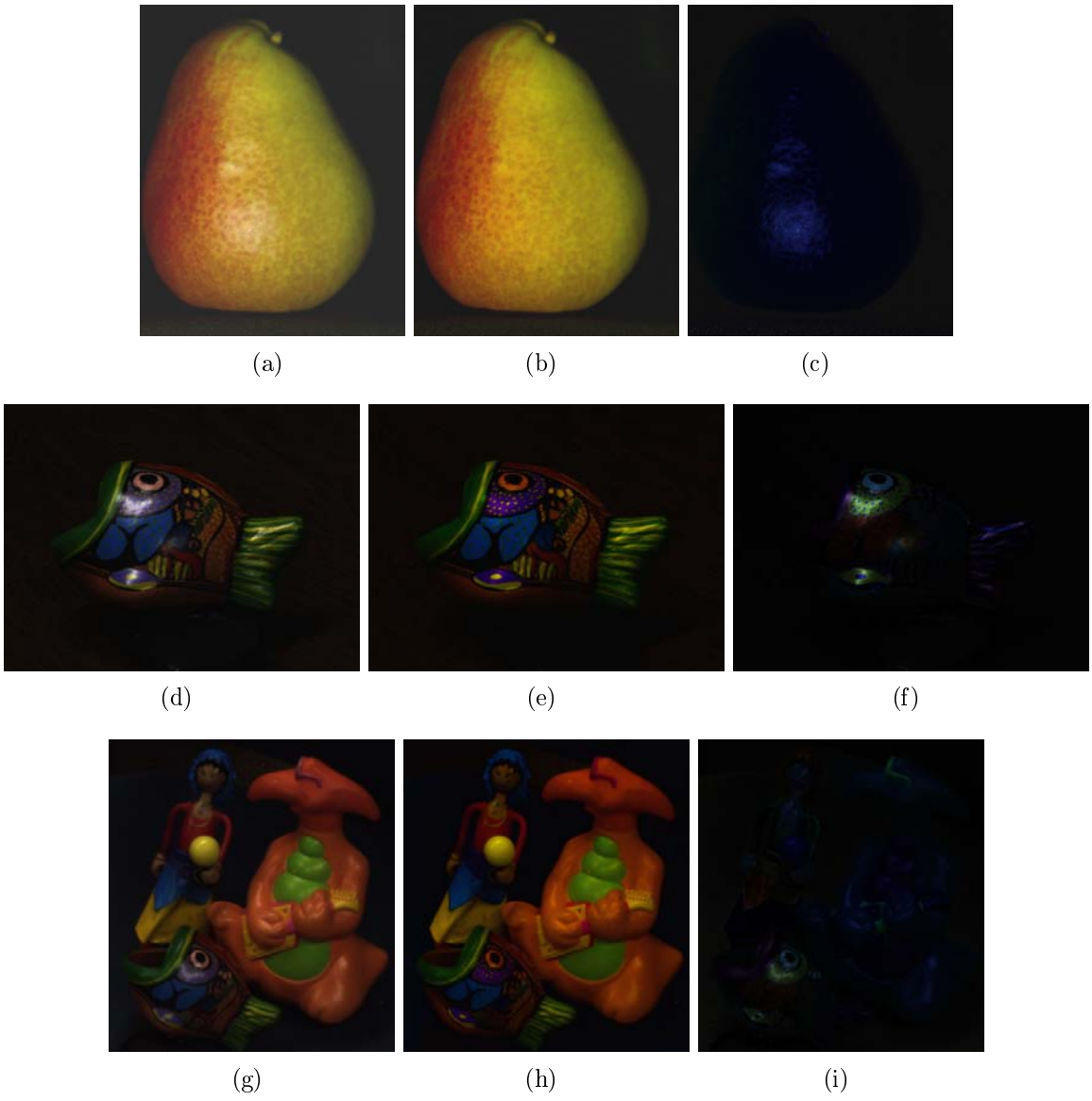

FIGURE 5. Reflection separation results of images having multicolor surfaces. (a), (d), (g) portrays the original input images. (b), (e), (h) the resulted diffuse reflectance, and (c), (f), (i) the specular reflectance of the input images respectively.

linear expression that separates a scene image into two distinct sets of image reflectance. The approach described relies solely on image color information of dichromatic surfaces without requiring segmentation procedures. Furthermore, by isolating the image diffuse reflectance distribution, we showed that image object geometry information can be recovered using the proposed specular reflectance shifting process. We evaluated our proposed method on several color images comprising uniform and multicolor surfaces. For uniform surfaces, the reflectance separation process can be achieved simply by shifting all specular reflectance image pixels toward the diffuse reflectance distribution using a single constant value for each of the image color channels. On the other hand, for multicolor surfaces, the shifting distance is processed independently for each specular reflectance pixel. An important next step is to explore the correlation of each specular reflectance component

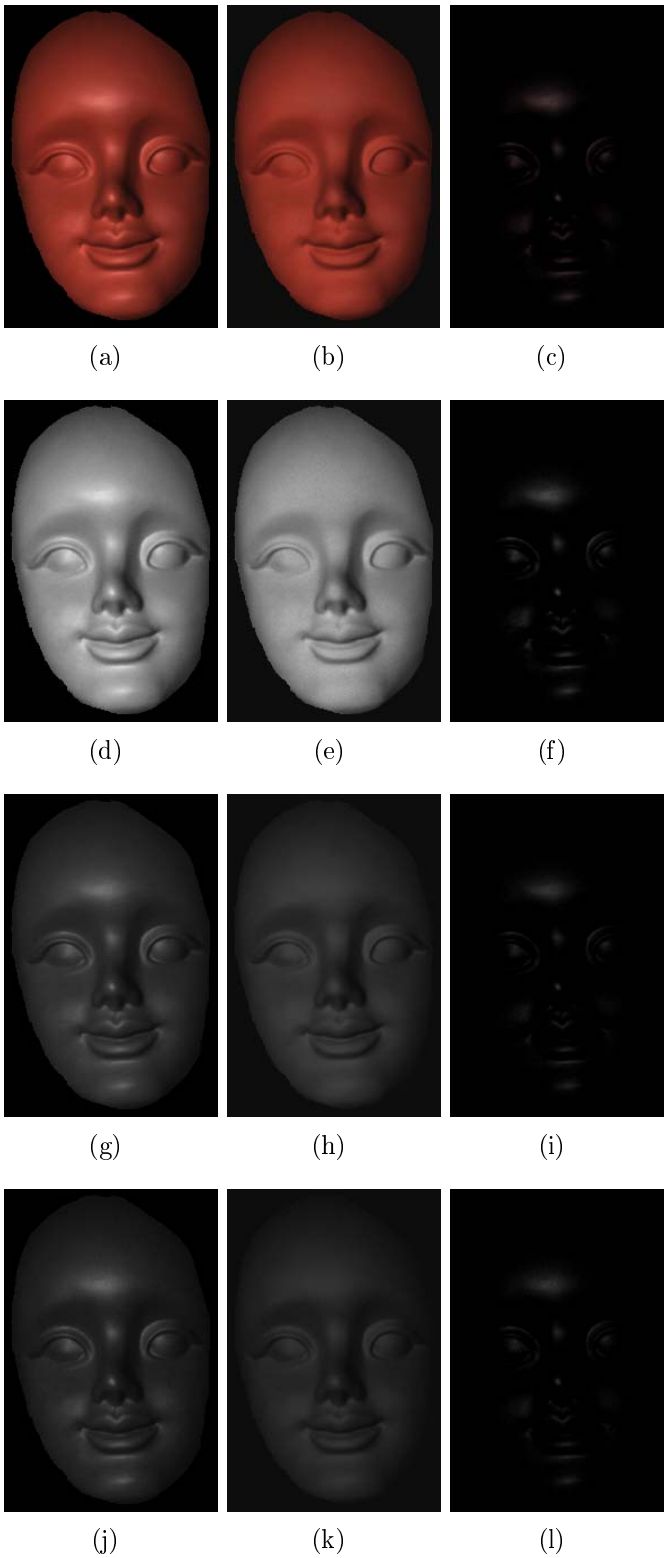

FIGURE 6. Reflection separation results "Red face front view" having a uniform color surface along RGB color channels. Row 2-4 represents color channels Red, Green and Blue respectively.

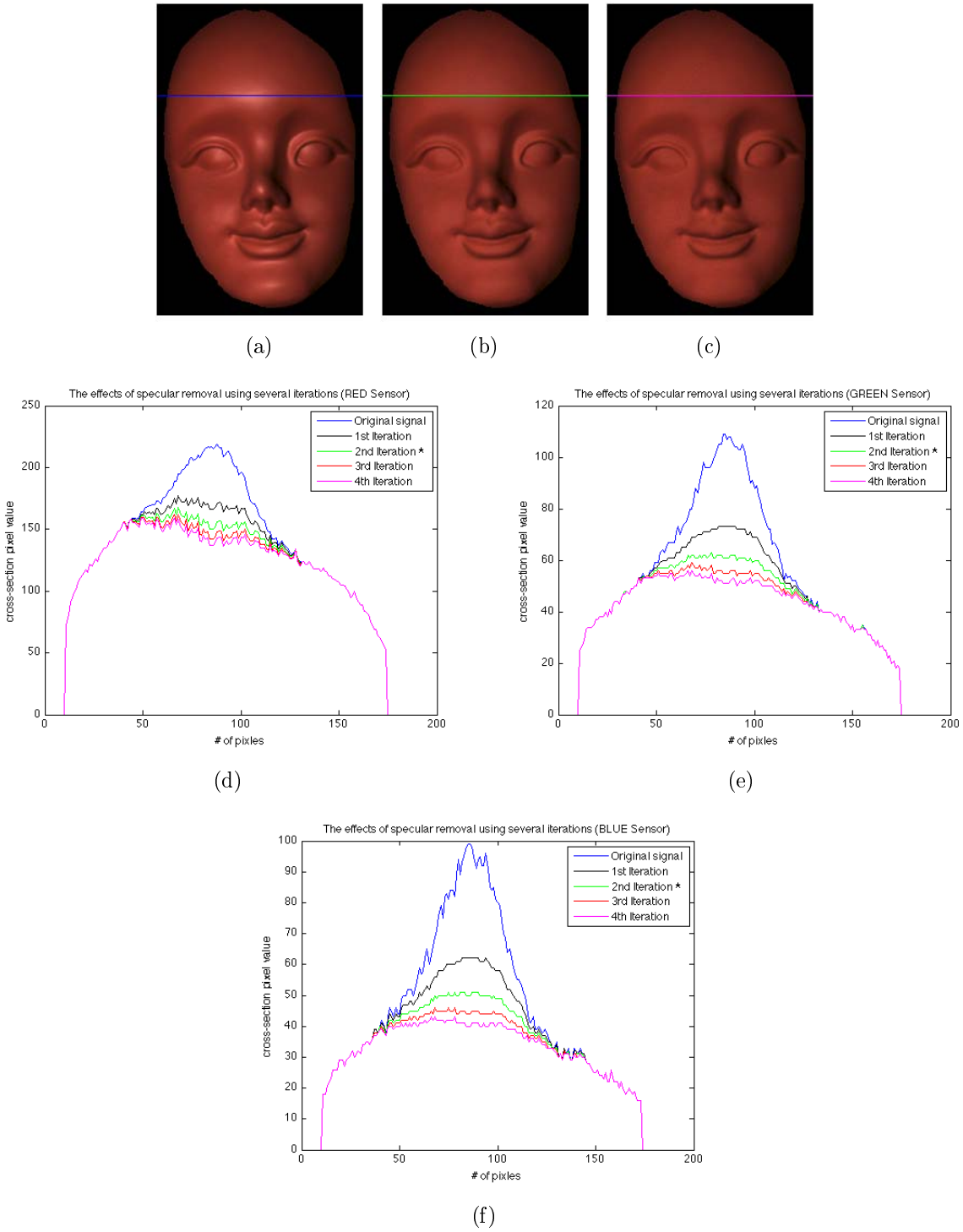

FIGURE 7. Specular removal process along the input image blue horizontal line. (a) Input image. (b) Input image after 2 iterations. (c) Input image after 4 iterations. (d) Cross-section of the image red channel for different iteration steps. (e) Cross-section of the image green channel for different iteration steps. (f) Cross-section of the image green channel for different iteration steps.

neighbor. A more precise shifting process can also be considered to correct highly textured image surfaces.

Acknowledgment. This work was supported by the National Science Foundation under grants CNS-0959985, HRD-0833093 and CNS-1042341. The authors are also grateful for the support provided by the Florida International University Graduate School through the Dissertation Year Fellowship.

REFERENCES

[1] T. T. Zin, H. Hama and S. S. Koh, Robust signboard recognition in the presence of occlusion and reflection, *International Journal of Innovative Computing, Information and Control*, vol.3, no.6(A), pp.1321-1334, 2007.

[2] L. Li and Y. Wang, A color image segmentation algorithm of adaptive selecting primary feature in multi color space, *ICIC Express Letters*, vol.5, no.9(B), pp.3297-3302, 2011.

[3] N. Araki, K. Nishiuchi, T. Sato, Y. Konishi, E. Fujiwara and H. Ishigaki, Defect detection for mirror polished metal surface using independent component analysis, *ICIC Express Letters*, vol.5, no.9(B), pp.3291-3296, 2011.

[4] S. Shafer, Using color to separate reflection components, *Color Research and Applications*, vol.10, no.4, pp.210-218, 1985.

[5] Y. Sato and K. Ikeuchi, Temporal-color space analysis of reflection, *Journal of the Optical Society of America A*, vol.11, 1994.

[6] S. Lin, Y. Li, S. B. Kang, X. Tong and H. Y. Shum, Diffuse-specular separation and depth recovery from image sequences, *Proc. of European Conf. Computer Vision*, pp.210-224, 2002.

[7] S. Lin and H. Y. Shum, Separation of diffuse and specular reflection in color images, *Proc. of IEEE Conf. Computer Vision and Pattern Recognition*, 2001.

[8] J. P. S. Parkkinen, J. Hallikainen and T. Jasskelainen, Characteristic spectra of munsell colors, *Journal of the Optical Society of America A*, vol.6, 1989.

[9] S. K. Nayar, X. S. Fang and T. Boult, Separation of reflection components using color and polarization, *International Journal of Computer Vision*, vol.21, no.3, 1996.

[10] Z. Zhang, S. Ren, T. Miyake, H. Fujiwara and T. Imamura, Processing reflections on metallic surfaces using a special random sampling method, *International Journal of Innovative Computing, Information and Control*, vol.4, no.7, pp.1595-1606, 2008.

[11] L. B. Wolff and T. Boult, Constraining object features using polarization reflectance model, *IEEE Trans. Pattern Analysis and Machine Intelligence*, vol.13, no.7, pp.635-657, 1991.

[12] G. J. Klinker, S. A. Shafer and T. Kanade, The measurement of highlights in color images, *International Journal of Computer Vision*, vol.2, pp.7-32, 1990.

[13] R. T. Tan and K. Ikeuchi, Separating reflection components of textured surfaces using a single image, *IEEE Transactions on Pattern Analysis and Machine Intelligence*, vol.27, pp.178-193, 2005.

[14] S. P. Mallick, T. Zickler, P. N. Belhumeur and D. J. Kriegman, Specularity removal in images and videos: A PDE approach, *IEEE European Conference on Computer Vision*, 2006.

[15] M. Khosravy, M. R. Asharif and K. Yamashita, A PDF-matched short-term linear predictability approach to blind source separation, *International Journal of Innovative Computing, Information and Control*, vol.5, no.11(A), pp.3677-3690, 2009.

[16] H. C. Lee, E. J. Breneman and C. P. Schulte, Modeling light reflection for computer color vision, *IEEE Transactions on Pattern Analysis and Machine Intelligence*, vol.12, no.4, pp.402-409, 1990.

[17] G. D. Finlayson and G. Schaefer, Solving for color constancy using a constrained dichromatic reflection model, *International Journal of Computer Vision*, vol.42, no.3, pp.127-144, 2001.

[18] S. Tominaga and B. A. Wandell, Standard surface-reflectance model and illumination estimation, *Journal of Optics Society of America A*, vol.6, no.4, pp.576-584, 1989.

[19] H. C. Lee, Method for computing the scene-illuminant from specular highlights, *Journal of Optics Society of America A*, vol.3, no.10, pp.1694-1699, 1986.

[20] M. Storring, H. J. Andersen and E. Granum, Estimation of the illuminant colour from human skin colour, *Proc. of the 4th IEEE International Conference on Automatic Face and Gesture Recognition*, pp.64-69, 2000.

[21] C. P. Huynh and A. Robles-Kelly, A solution of the dichromatic model for multispectral photometric invariance, *International Journal of Computer Vision*, vol.40, no.1, pp.1-27, 2010.

[22] S. Tominaga and Y. Moruchi, Principal component analysis-based reflectance analysis/synthesis of cosmetic foundation, *The Journal of Imaging Science and Technology*, vol.53, no.6, 2009.
[23] J. W. Park and K. H. Lee, Inpainting highlights using color line projection, *IEICE Transactions on Information Systems*, vol.E90D, pp.250-257, 2007.
[24] T. Zickler, P. Mallick and D. J. Kriegman, Color subspaces as photometric invariants, *International Journal of Computer Vision*, vol.79, pp.13-30, 2008.
[25] R. T. Tan, K. Nishino and K. Ikeuchi, Separating reflection components based on chromaticity and noise analyses, *IEEE Transactions on Pattern Analysis and Machine Intelligence*, vol.26, pp.1373-1979, 2004.
[26] K. Yoon and I. S. Kweon, Correspondence search in the presence of specular highlights using specular-free two band images, *Proc. of Asian Conference on Computer Vision*, pp.761-770, 2006.
[27] R. T. Tan, K. Nishino and K. Ikeuchi, Color constancy through inverse-intensity chromaticity space, *Journal of the Optical Society of America A*, vol.21, no.3, pp.321-334, 2004.
[28] S. Mallick, T. Zickler, D. Kriegman and P. Belhumeur, Beyond lambert: Reconstructing specular surfaces using colors, *IEEE Conference on Computer Vision and Pattern Recognition*, vol.II, pp.619-626, 2005.